Appendix A. Supplementary material

Table A.4 provides a list of frequently used acronyms and their definitions.

Appendix A.1. Oher biomarkers for AD, PD and DLB

This supplementary section contains additional information regarding the use of additional biomarkers for the diagnosis of AD, PD, and DLB.

Appendix A.1.1. Methods

As indicated in section 2.1, in some cases additional biomarkers were used in the diagnostic process. These included presynaptic dopaminvergic imaging (DAT SPECT or Fdopa PET), evalutation of cerebral amylooid deposits with PiB PET, and analysis of the cerebral spinal fuild (CSF) for Aβ42, t-Tau, and p-Tau. PiB PET and DAT SPECT or Fdopa PET scans were evaluated visually by a nuclear medicine physician as part of a routine clinical investigation.

For CSF, Aβ42 was considered abnormal at $>$ 500 pg/mL, t-Tau $>$ 350 pg/mL, and p-Tau $>$ 85 pg/mL.

The profile was considered abnormal when t-Tau and/or p-Tau levels were elevated, and/or Aβ42 levels were decreased. In a typical AD profile, t-tau and p-tau levels are increased, and Aβ42 levels are decreased. An elevated p-tau combined with a decreased Aβ42 can be used to support the diagnosis AD [1]. If the CSF profile was not typical, PiB PET was usually performed to confirm the diagnosis.

Appendix A.1.2. Results

All information concerning the biomarkers each cohort is included in table A.5. In all subjects, structural imaging was performed (also see section 2.1).

In AD patients in the *reference* cohort, PiB PET was performed in a total of 13 out of 20 cases, all of which were positive. In 12 out of 20 cases, CSF analysis was performed. Ten cases had an abnormal CSF profile, but only 5 had a typical profile. In the other cases, the profile was not typical (usually because Aβ42 was borderline-normal). In all of these 10 cases, a PiB PET was performed, which was positive and could support the clinical diagnosis. In 2 cases, the CSF was normal. In one, a PiB PET could also confirm the diagnosis. In one case, a PiB PET was not performed but the clinical picture was compatible with AD and there was a clear progression on clinical follow-up and neuropsychological evaluation.

In AD patients in the *evaluation* cohort, PiB PET was performed in most cases (31/36). In all of these cases, there was abnormal PiB accumulation compatible with AD. In one case, the clinical diagnosis was AD and no additional biomarker (CSF or PiB PET) was performed. CSF analysis was performed in 19/36 cases, and was abnormal in 16 cases. In 3 cases, all three markers were abnormal; in two of these a PiB PET scan was also performed, which was indeed compatible with AD. In 13 cases, the CSF profile was not entirely typical (again, usually because Aβ42 was borderline-normal). In all but one of those cases, the PiB PET was compatible with AD. In one, it was not performed.

In patients with *DLB*, the diagnosis was made mostly on clinical characteristics according to the McKeith criteria [2]. Additional biomarkers were applied in the minority (9/23). Presynaptic dopaminergic imaging was performed in 5/23 cases (all 5 were abnormal). PiB PET was performed in 7 cases, of which one was graded abnormal. This could signify a mixed AD-DLB profile. CSF analysis was performed in 4 cases; 1 was compatible with AD, 1 was uncertain, and 2 were normal.

In *PD*, presynaptic dopaminergic imaging was performed in 9 out of 20 patients in the reference cohort, and 12/21 in the evaluation cohort. Per definition, presynaptic dopaminergic imaging was abnormal in these PD cases.

Appendix A.1.3. Medication status during FDG-PET acquisition

In PD, there is relative hypermetabolism in the posterior putamen, globus pallidus, ventral thalamus and dorsal pons. PD patients are usually treated with levodopa and levodopa therapy causes a normalization of relative hyperactivation of these areas. It has also been shown that PDRP z-scores decrease after levodopa therapy [3]. In our cohort, levodopa was not routinely withheld during FDG-PET scanning. Therefore, glucose metabolism might be altered in patients in the 'on' versus the 'off' levodopa state, which could have influenced our results. In table A.5, we have indicated how many patients were scanned 'on' or 'off'.

Acronyms	Definitions
AD	Alzheimer's Disease
PD	Parkinson's Disease
HC	Healthy Control
DLB	Dementia with Lewy Bodies
(i)RBD	(idiopathic) REM (Rapid Eye Movement) sleep Behaviour Disorder
SSM/PCA	Subprofile Model and Principal Component Analysis
PDRP	Parkinson's Disease Related Pattern
ADRP	Alzheimer's Disease Related Pattern
LVQ	Learning Vector Quantization
GMLVQ	Generalized Matrix Learning Vector Quantization

Table A.4: Table of frequently used acronyms and their definitions.

Appendix A.2. Additional GMLVQ results

This supplementary section includes additional results belonging to the GMLVQ model(s). In fig. A.8 the average (obtained from the cross-validation procedure, see section 2.5) diagonal of the relevance matrix is shown. These values indicate the relevance of each of the PCs for the classification of AD, DLB, HC, and PD.

In the fig. A.9 the average eigenvalues and eigenvalues of the projection plots are provided. These plots show that the first three contribute most to the discriminative space.

Figure A.10 contains the voxel representation of the third eigenvector, see section 2.5.1 and section 3.

	Dopaminergic imaging (n)	PiB PET (n)	CSF performed (n)	No additional biomarker	Dopaminergic medication
PD (n=20)	9	0	0	11	3 ON 17 OFF
AD (n=20)	0	13 (all positive)	12 (10 abnormal)	5	n/a

(a) Reference cohort.

	Dopaminergic imaging (n)	PiB PET (n)	CSF performed (n)	No additional biomarker	Dopaminergic medication
PD (n=21)	12 (all abnormal)	0	0	9	14 ON, 7 OFF
AD (n=36)	0	31 (all positive)	19 (16 abnormal)	1	36 OFF
DLB (n=23)	5 (all abnormal)	7 (1 positive)	4 (2 abnormal)	14	4 ON, 5 OFF, 10 n/a
RBD (n=21)*	17 (9 abnormal)	0	0	n/a	20 OFF

(b) Evaluation cohort.

Table A.5: Additional biomarkers. * For a more thorough description of this cohort we refer to [4, 5].

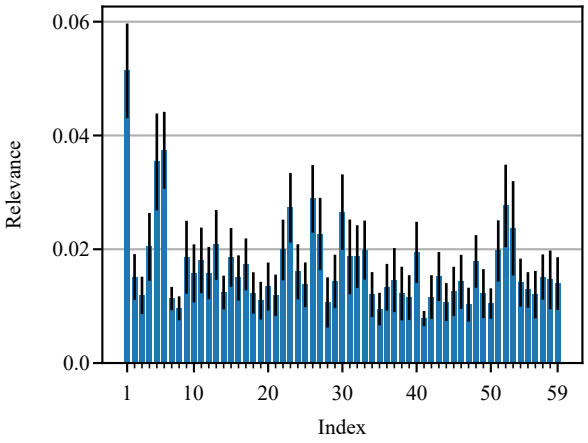

Figure A.8: Average diagonal (with standard deviation) of the relevance matrix (relevance profile). The index on the x-axis match the PCs constructed from the reference group (section 2.4).

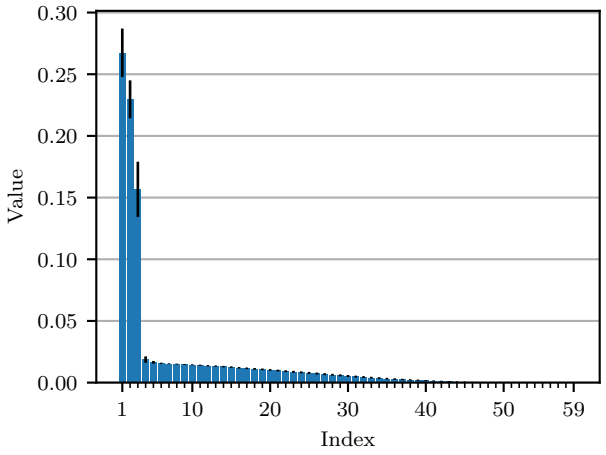

(a) Average eigenvalues extracted from the ten times repeated ten-fold cross-validation procedure.

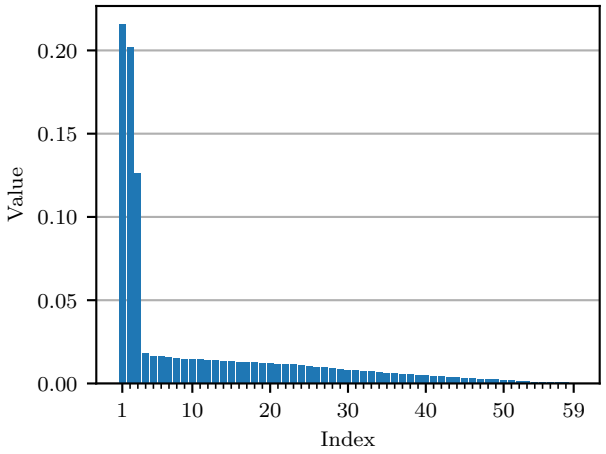

(b) Eigenvalues resulting from the decomposition of the average relevance matrix.

Figure A.9: Eigenvalues of the cross-validation process and resulting from the decomposition of the average relevance matrix.

References

[1] N. S. M. Schoonenboom, F. E. Reesink, N. A. Verwey, M. I. Kester, C. E. Teunissen, P. M. van de Ven, Y. A. L. Pijnenburg, M. A. Blankenstein, A. J. Rozemuller, P. Scheltens, W. M. van der Flier, Cerebrospinal fluid markers for differential dementia diagnosis in a large memory clinic cohort, Neurology 78 (1) (2012) 47–54. doi:10.1212/wnl.0b013e31823ed0f0.

[2] I. G. McKeith, B. F. Boeve, D. W. Dickson, G. Halliday, J.-P. Taylor, D. Weintraub, D. Aarsland, J. Galvin, J. Attems, C. G. Ballard, et al., Diagnosis and management of dementia with lewy bodies: fourth consensus report of the dlb consortium, Neurology 89 (1) (2017) 88–100.

[3] K. Asanuma, Network modulation in the treatment of parkinson's disease, Brain 129 (10) (2006) 2667–2678. doi:10.1093/brain/awl162.

[4] R. V. Kogan, A. Janzen, S. K. Meles, E. Sittig, R. J. Renken, V. Gurvits, G. Mayer, K. L. Leenders, W. H. Oertel, R. W. Group, et al., Four-year follow-up of [18f] fluorodeoxyglucose positron emission tomography–based parkinson's disease–related pattern expression in 20 patients with isolated rapid eye movement sleep behavior disorder shows prodromal progression, Mov. Disord. 36 (1) (2020) 230–235.

[5] A. Janzen, R. V. Kogan, S. K. Meles, E. Sittig, R. J. Renken, F. F. Geibl, J. Booij, G. Stormezand, M. Luster, G. Mayer, K. L. Leenders, W. H. Oertel, Rapid eye movement sleep behavior disorder: abnormal cardiac im-

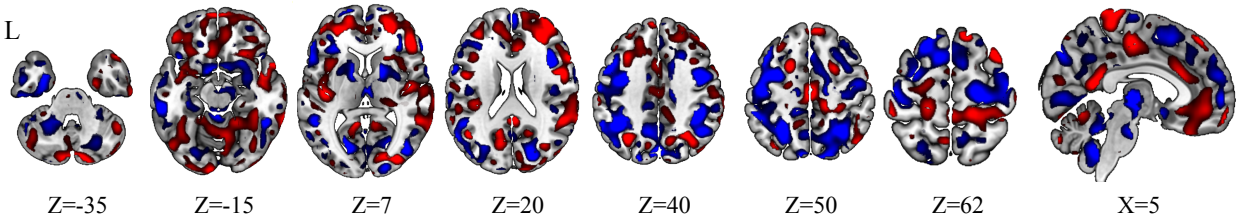

Figure A.10: Voxel representation (pattern) of the third eigenvector of the relevance matrix constructed by GMLVQ. The values indicate activation above or below the average healthy control from the *reference* group (table 1a). To aid visualization, each voxel in these 3D images was z-transformed and overlaid on a T1 MRI brain template. Images were arbitrarily thresholded at $|z > 0.5|$ to remove near-zero values.

age and progressive abnormal metabolic brain pattern, Mov. Disord. 37 (3) (2022) 624–629. doi:10.1002/mds.28859.